Research Article **Open Access**

Systemic Delivery of Thiol-Specific Antioxidant hPRDX6 Gene by AAV2/8 Inhibits Atherogenesis in LDLR KO Mice on HCD

Zhu HQ, Cao M, Straub KD and Hermonat PL*

Central Arkansas Veterans Healthcare System, 111J, 4300 West 7th Street, Little Rock, AR 72205, USA, Division of Cardiology, University of Arkansas for Medical Sciences and VA Medical Center, Little Rock, AR 72205, USA

Abstract

Atherosclerosis is an inflammatory disorder of arteries and reactive oxygen species (ROS) have been implicated as a major etiology. Various anti-ROS genes, such as superoxide dismutates and catalase, have been studied by gene transfer for their abilities to limit a variety of ROS-related cardiovascular injuries such as balloon-induced and ischemia-reperfusion injury. However the thiol-ROS compartment has never been explored by gene therapy/ gene delivery for potential therapeutic intervention. Human peroxiredoxin 6 (hPRDX6, AOL2) is fully unique in that in addition to its thiol-specific anti-oxidant ability it has a coupled phospholipase A2 catalytic domain. Here we delivered hPRDX6, expressed by the cytomegalovirus immediate early promoter (CMV), by systemic pseudotyped adeno-associated virus 2/8 (AAV2/8) gene transfer into low density lipoprotein receptor knockout mice on high cholesterol diet (LDLR KO HCD). It was found that AAV2/8/hPRDX6 gene delivery and expression inhibited systolic blood velocity, aortic cross sectional area, and aortic wall thickness compared to Neo-HCD control, consistent with reduced atherosclerosis. Markers of macrophages/foam cells, CD68, ITGAM, EMR, verified lower atherosclerosis, as all were lower in the AAV8/hPRDX6-HCD-treated animals compared to Neo-HCD controls, analyzed by either quantitative reverse transcriptase polymerase chain reaction amplification or by immuno-histochemistry, or both. Analysis of the immune state of the aortas (Th1 or Th2 cytokine expression) revealed nothing significant, with only IL-10 expression being lower in PRDX6-treated animals. This study, for the first time, demonstrated that hPRDX6 gene delivery, augmenting endogenous mouse (m)PRDX6 expression, giving therapeutic benefit against HCD-driven atherosclerosis and suggests further studies of PRDX6, and related anti-thiol-ROS approaches, is warranted.

Keywords: Antioxidant enzyme; Phospholipase A2; Adeno-associated virus; Gene therapy; Mouse knockout; Atherosclerosis

Introduction

Reactive oxygen species (ROS) are present in all cells and are eliminated by antioxidants. However when produced in excess, overpowering the resident antioxidant defenses, oxidative stress takes place. ROS is produced by a variety of cellular metabolisms, in particular mitochondrial respiration [1]. Sometimes ROS acts as intracellular signaling molecules [2], but ROS is very important because of the widespread damage it can cause to cellular proteins [3], DNA [4], and lipids [5]. ROS is a factor in almost all diseases of aging, and its role in cardiovascular disease is well documented [6,7]. Our interest has been in controlling ROS's contributions to atherogenesis. ROS appears to be a factor in the earliest stage of atherosclerosis, the activation of endothelial cells, leading to their dysfunction [8-10]. Adhesion molecules are up-regulated which leads to the recruitment of monocytes, macrophages and other inflammatory cells. These recruited cells promote the generation of lipid engorged foam cells and the proliferation of vascular smooth muscle cells, both hallmarks of atherosclerosis. Clinical studies also support ROS being a significant contributor to atherosclerosis [11,12].

For defense the cell encodes many anti-oxidant genes including various superoxide dismutases (SODs), glutathione peroxidases (GPXs), catalases, glutaredoxins. thioredoxin peroxidases (peroxiredoxins), and others. However, while the cell has many counteracting genes against ROS it is also therapeutically possible to enhance these resident defenses. While anti-oxidant diets might be tried, gene therapy may be another approach which would give a more permanent treatment [13,14]. For example adeno-associated virus (AAV), first used in 1984 [15-17], is known to actively express transduced genes for 22 months in mice and 10 years in humans [18,19]. Gene delivery/gene therapy, utilizing a variety of virus types, has delivered antioxidant genes into

cells and animals, however most of these studies have limited to the delivery of various forms of SOD or catalase [20-28].

Each anti-ROS protein is usually concentrated within a specific cellular compartment and metabolizes specific forms of ROS. We have interest in thiol-specific antioxidant peroxiredoxin 6 (PRDX6) and its potential as an anti-ROS therapeutic gene. There are six mammalian members of the peroxiredoxin family and PRDX6 is the only one which has a single conserved cysteine residue (all others have 2) and does not use thioredoxin as a reductant [29-31]. Also unusual among the peroxiredoxin family, PRDX6 has Ca2+-independent phospholipase A2 (PLA2) activity. The PLA2's role is protective against lipid peroxidation and resulting cell death/lysis. Thus PRDX6, having two active domains in close proximity to one another, is a very unique protein. Moreover PRDX6, while present in the cytosol, has also sometimes been reported in the nucleus [32]. Thus PRDX6 appears to be within and potentially protects multiple significant compartments of the cell. Here we demonstrate that human (h) PRDX6 gene delivery by AAV8 capsid inhibits the development of atherosclerosis in low density lipoprotein receptor knockout mice on high cholesterol diet (LDLR KO HCD) and lowers macrophage accumulation.

---

*Corresponding author: Paul L Hermonat, Central Arkansas Veterans Healthcare System, 111J, 4300 West 7th Street, Little Rock, AR 72205, USA, Division of Cardiology, University of Arkansas for Medical Sciences and VA Medical Center, Little Rock, AR 72205, USA, E-mail: plhermonat@uams.edu

Materials and Methods

AAV vector construction and virus generation

The human (h) PRDX6 was obtained from Open Biosystems and was ligated behind the cytomegalovirus immediate early promoter within the gutted AAV vector dl3-97 to generate AAV/hPRDX6. The AAV/Neo vector has been described previously [33,34]. Virus was produced using pDG8 helper and tittered by dot blot analysis by standard methodologies.

Animal treatments

LDLR KO mice (B6; 129S7-*Ldlr^tm1Her*/J) were obtained from Jackson Laboratories (Bar Harbor, ME, USA). Three groups of male mice (N=10), at 8 weeks old, were injected with 200 μl of AAV/Neo or AAV/hPRDX6 virus, at a titer of 1×10^{10} eg/ml, via tail vein. Two booster injections were given at intervals of 5-6 days. After virus injection a high cholesterol diet (HCD) of 4% cholesterol and 10% Coco butter diet (Harlan Teklad, Madison, Wis, USA) was maintained throughout the experiment. Another control group of mice were fed a normal diet. All experimental procedures conform to protocols approved by the Institutional Animal Care and Usage Committee of the Central Arkansas Veterans Health Care System at Little Rock.2.3.

High resolution ultrasound imaging

A Vevo 770 High-Resolution Imaging system (Visualsonics, Toronto, Canada) with a RMV 707B transducer was used to examine aortic structures and blood velocity. Each mouse was first anesthetized by inhalation of 1.5% isoflurane (Isothesia, Abbot Laboratories, Chicago, USA) along with oxygen and then placed supine on a thermostatically heated platform for maintenance of a constant body temperature. Their legs were taped to ECG electrodes for cardiac function monitoring. A chemical hair remover (Church & Dwight Co., Inc., NJ, USA) was used to remove abdominal hair. A gel (Medline Industries, Inc., Mundelein, USA) was then spread over the skin as a coupling medium for the transducer. Image acquisition was initiated on B-mode; two levels of the vessel were visualized longitudinally: thoracic region and renal region. After that a short-axis view was then immediately taken to visualize the same arterial site in a cross sectional view. Individual frames and cine loops (300 frames) were acquired at each level and recorded at distances of 1mm throughout the length of the aorta. Using both the longitudinal and transverse images, measurements and data analysis was performed off line using the customized version of Vevo 770 Analytical Software.

Tissue sampling and processing

After 20 weeks post virus injection with continuous HCD, mice were euthanized by CO_2 exposure and exsanguinations were done for blood collection. Entire aorta was prepared as described earlier for immuno-histochemical analysis [33]. Aorta were first flushed with saline solution and fixed in 10% neutral-buffered formalin (Sigma, St Louis, MO, USA). At 24hours post-fixation the tissue was embedded by paraffin and sectioned using a microtome. Additional aorta tissues were frozen in liquid nitrogen and stored in -80°C for RNA or protein isolation.

Measurement of plasma cholesterol

Total plasma cholesterol of control, AAV/Neo and AAV/hPRDX6-treated mice were measured by VetScan VS2 (Abaxis, Union City, CA, USA) at the Veterans Animal Laboratory (VAMU).

RNA isolation and real-time qRT-PCR.

Total RNA from aortas was extracted using Trizol reagent (Invitrogen Carlsbad, CA) and was treated with DNase I (Invitrogen, Carlsbad, CA). cDNA was then synthesized using oligo(dT)$_{18}$ primers and RNase H-reverse transcriptase (Invitrogen, Carlsbad, Calif) according to the manufacturer's instructions. Integrated DNA Technologies, Inc. (Coralville, IA) synthesized the primers for qPCR analysis (Table 1). Quantitative real-time polymerase chain reaction (qRT-PCR) was performed using SYBR Green PCR Master Mix kit, using an Applied Biosystems Fast 7900HT real-time PCR system (Applied Biosystems, Foster City, CA). The results were then analyzed by SDS 2.3 software.

Western blot analysis

Total proteins were extracted from the homogenized liver in the T-PER tissue protein extraction reagent (Thermo Scientific). Protein concentration was determined using the protein assay dye reagent (Bio-RAD) and were normalized for equal loading. After separating on 10% SDS-PAGE gels, protein was transferred to polyvinylidene difluoride membranes. The membranes were then blocked for 1 hour at room temperature with 5% nonfat milk in $1 \times$ TBST buffer (10 mM Tris-Cl (pH 7.5), 150 mM NaCl, 0.1% Tween 20). Followed a brief rinse, membranes were incubated with primary monoclonal antibody specific to PRDX6 (1:1000 dilution, Sigma-Aldrich) at 4 °C overnight and with a secondary horseradish-peroxidase (HRP)-conjugated antibody (1:2000 dilution, Sigma-Aldrich) for 1 h at room temperature. Washes in $1 \times$ TBST buffer were performed between incubations for three times. Blots were developed with Pierce® ECL system (Thermo-Fisher Scientific). Probe detection of β-actin was carried out as control.

Results

AAV8 capsid delivers hPRDX6

To investigate the use of PRDX6 we utilized the LDLR KO mouse which develops atherosclerosis when placed on HCD. The human (h) PRDX6 gene was ligated behind the cytomegalovirus immediate early (CMV) promoter within a gutted AAV vector, dl3-97. Pseudotyped AAV2/8 virus was produced using pDG8 (obtained from Zolohukin,
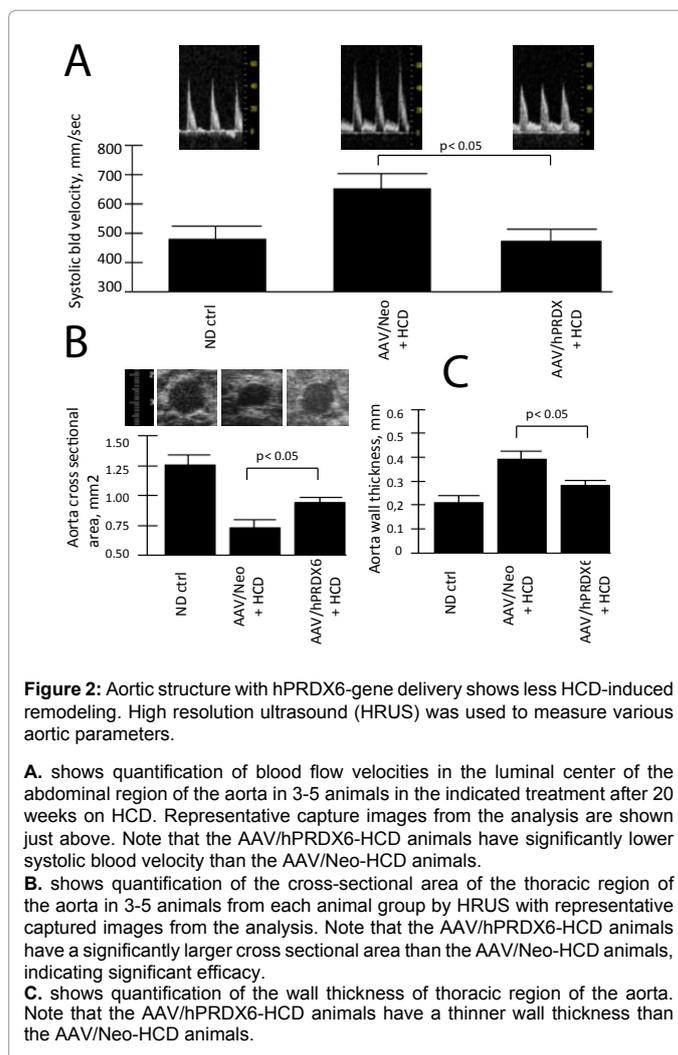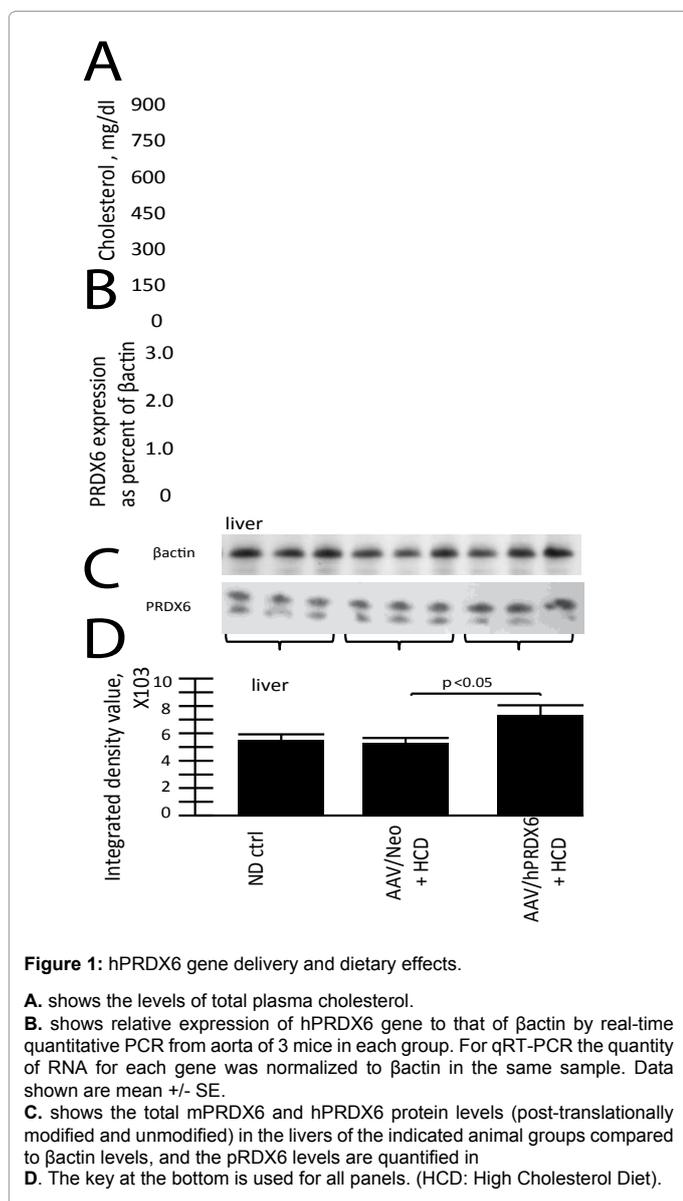
GENE	polarity	5' 3
Bactin	sense	ATCTGGCACCACACCTTCTAC
	antisense	GAAGGTCTCAAACATGATCTGG
PRDX6	sense	ATCATCGATGATAGGAATC
	antisense	CTTCAGCTTCTTATCAGGA
EMR	sense	AAGTATTCCAACTGCTCT
	antisense	ATTGGCCCTCCTCCACTA
ITGAM	sense	TCCAGAGGCTGTGAATAT
	antisense	CTTCTGAAAGTCAATGTTGT
COL1A2	sense	CGTTCCCAAAGATGGTAGAT
	antisense	AGCCACCTCCGCTGACACCA
IL-4	sense	ATGTGCCAAACGTCCTCACA
	antisense	AGAACACTAGAGTTCTTCTT
IL-7	sense	AAATGACAGGAACTGATAGT
	antisense	GACATTGAATTCTTCACTGA
IL-10	sense	TACAGCCGGGAAGACAATAA
	antisense	AAGGAGTCGGTTAGCAGTAT
IL-12	sense	AGAATCACAACCATCAGCAG
	antisense	TTCACTCTGTAAGGGTCTGC

Table 1: Primer sequences. Shown are the indicated primer sets used to analyze gene expression by QRT-PCR.

U Florida). Figure 1A shows that those animals (Neo- and hPRDX-treated) placed on HCD had higher plasma levels of cholesterol than those on ND. Figure 1B demonstrates that the AAV8 vector successfully delivered and expressed the hPRDX6 vector into the aortas using tail vein injection, and expression was shown to be 1.7% that of βactin expression in the aorta. Figure 1C shows a western blot of PRDX6 protein in the liver of the various groups. Figure 1D shows a quantification of that data, and indicates the AAV/CMV-hPRDX6-treated animals had significantly higher PRDX6 protein expression than in the other groups. It should be noted that the anti-PRDX6 antibody we used recognizes both human and mouse forms (there are no human-specific anti-PRDX6 antibody available.

hPRDX6 inhibits HCD-induced arterial changes

We next analyzed the structures and blood kinetics of the various treated aortas by high resolution ultrasound (HRUS). Systolic blood velocity is perhaps the best, easiest, most reliable method for analyzing the extent of atherosclerosis by HRUS. Figures 2A demonstrate that

Figure 1: hPRDX6 gene delivery and dietary effects.

A. shows the levels of total plasma cholesterol.
B. shows relative expression of hPRDX6 gene to that of βactin by real-time quantitative PCR from aorta of 3 mice in each group. For qRT-PCR the quantity of RNA for each gene was normalized to βactin in the same sample. Data shown are mean +/- SE.
C. shows the total mPRDX6 and hPRDX6 protein levels (post-translationally modified and unmodified) in the livers of the indicated animal groups compared to βactin levels, and the pRDX6 levels are quantified in
D. The key at the bottom is used for all panels. (HCD: High Cholesterol Diet).

Figure 2: Aortic structure with hPRDX6-gene delivery shows less HCD-induced remodeling. High resolution ultrasound (HRUS) was used to measure various aortic parameters.

A. shows quantification of blood flow velocities in the luminal center of the abdominal region of the aorta in 3-5 animals in the indicated treatment after 20 weeks on HCD. Representative capture images from the analysis are shown just above. Note that the AAV/hPRDX6-HCD animals have significantly lower systolic blood velocity than the AAV/Neo-HCD animals.
B. shows quantification of the cross-sectional area of the thoracic region of the aorta in 3-5 animals from each animal group by HRUS with representative captured images from the analysis. Note that the AAV/hPRDX6-HCD animals have a significantly larger cross sectional area than the AAV/Neo-HCD animals, indicating significant efficacy.
C. shows quantification of the wall thickness of thoracic region of the aorta. Note that the AAV/hPRDX6-HCD animals have a thinner wall thickness than the AAV/Neo-HCD animals.

AAV/hPRDX6-HCD treated mice had significantly lower systolic blood velocity than AAV/Neo-HCD treated mice. Moreover, the systolic blood velocity of these mice was statistically similar to untreated ND controls. We went on further to measure the structural parameters of the aortas by HRUS and in Figures 2B it is found AAV/hPRDX6-HCD treated mice had significantly larger cross aortic cross sectional areas than AAV/Neo-HCD treated mice. Finally, HRUS analysis was used to analyze the aortic wall thickness. Figure 2C documents that AAV/hPRDX6-HCD treated mice had significantly thinner walls than AAV/Neo-HCD treated mice. These data, systolic blood velocity, aortic cross sectional area, and aortic wall thickness are all consistent and mutually supportive, all indicating that the hPRDX6 gene delivery was effective in limiting atherogenesis under the conditions of HCD in the LDLR KO mouse.

hPRDX6 inhibits arterial macrophage accumulation

Using Q-RTPCR analysis, Figures 3A and 3B show that two markers of macrophages, EMR and ITGAM, were significantly lower (EMR), or trended lower (ITGAM) in AAV/hPRDX6-HCD treated mice compared to AAV/Neo-HCD treated mice. Additional analysis of aortic tissue by immuno-histochemistry for ITGAM and CD68, Figures 3C and 3D, both marker of macrophages were consistent the QRT-PCR data, both showing lower macrophage/foam cell levels being

lower in AAV/hPRDX6-HCD treated mice than AAV/Neo-HCD treated mice. These data are fully consistent with the Visualsonics-derived HRUS analysis (Figure 2), all consistent with hPRDX6-treated animals being resistant to HCD-induced atherogenesis compared to Neo-treated animals.

PRDX6 delivery does not significantly change aortal immune status

While macrophage (foam cell) accumulation was inhibited we assess the overall immune status of the aortas by cytokine expression. QRT-PCR analysis was used to address this question, first focusing on Th1 response cytokines. The aortas of 3 members of each group were used to isolate mRNA was isolated from of each group and were analyzed for IL-12 expression (Figure 4A). However, IL-12 levels were essentially unchanged in hPRDX6-HCD treated animals than Neo-HCD treated. Analysis of IL-7, another Th1 cytokine, gave similar results (Figure 4B). We next analyzed Th2 cytokines and figure 4C shows a QRT-PCR analysis of IL-4 expression in the aortas of the three animal groups. Yet again, and now for Th2 response, IL-4 levels were unchanged among the three animal groups. Finally we analyzed for IL-10 expression, a final Th2 response cytokine, by QRT-PCR. This time the IL-10 levels were found to be significantly lower in hPRDX6-HCD treated animals than Neo-HCD treated. Yet, this isolated change, unsupported by IL-4, we believe is unremarkable (Figure 4D).

Collagen expression in aortas

Finally we analyze whether collagen expression/fibrosis might be significantly altered by hPDRX6 gene delivery. QRT-PCR analysis of COL1A2 expression in the aortas was undertaken (Figure 5) and, as
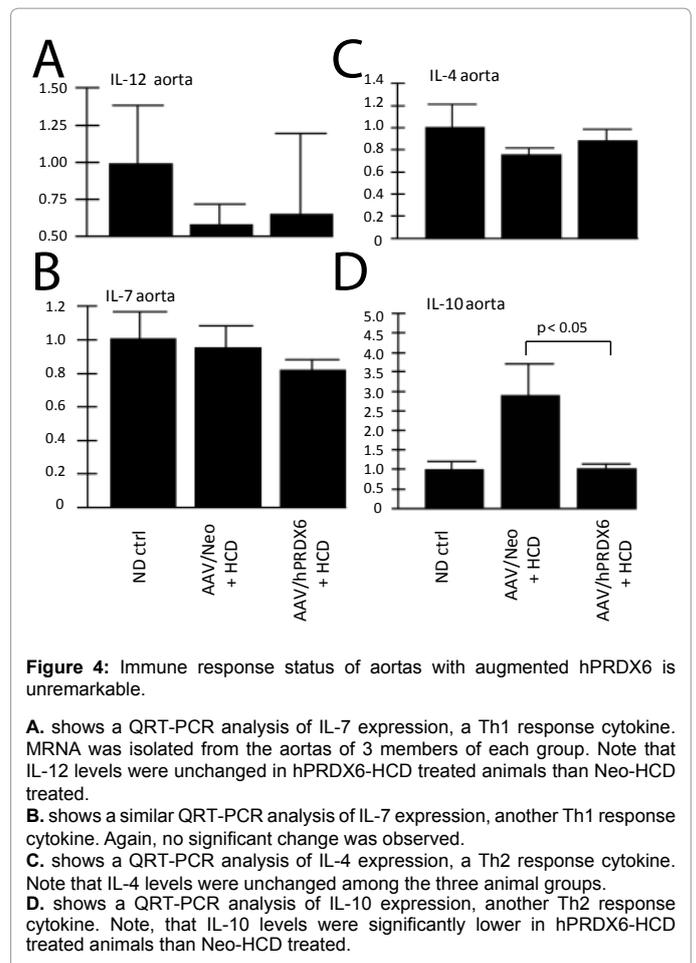

Figure 4: Immune response status of aortas with augmented hPRDX6 is unremarkable.

A. shows a QRT-PCR analysis of IL-7 expression, a Th1 response cytokine. MRNA was isolated from the aortas of 3 members of each group. Note that IL-12 levels were unchanged in hPRDX6-HCD treated animals than Neo-HCD treated.

B. shows a similar QRT-PCR analysis of IL-7 expression, another Th1 response cytokine. Again, no significant change was observed.

C. shows a QRT-PCR analysis of IL-4 expression, a Th2 response cytokine. Note that IL-4 levels were unchanged among the three animal groups.

D. shows a QRT-PCR analysis of IL-10 expression, another Th2 response cytokine. Note, that IL-10 levels were significantly lower in hPRDX6-HCD treated animals than Neo-HCD treated.
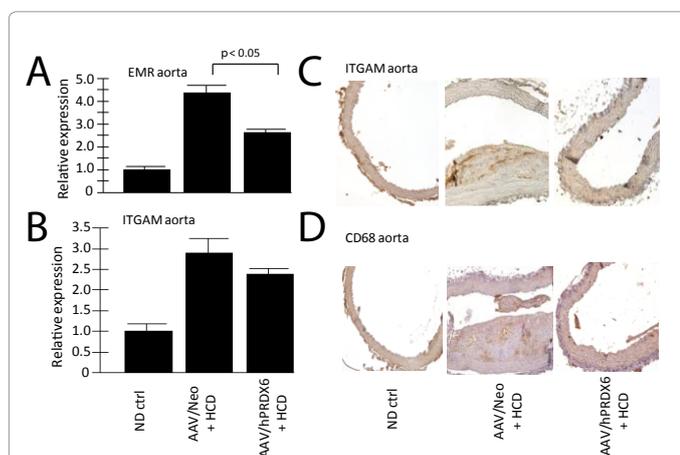

Figure 3: Macrophage burden of aortic tissue is down with hPRDX6 gene treatment.

A. shows a QRT-PCR analysis of EMR expression, a marker of macrophages, in the aorta using mRNA from three different animals from each indicated group Note, macrophage levels were significantly lower ($p < 0.05$) in hPRDX6-HCD treated animals than Neo-treated.

B. shows a similar QRT-PCR analysis of ITGAM expression, another macrophage marker. Note, again, macrophage levels trended lower in hPRDX6-HCD treated animals than Neo-treated.

C. shows an immuno-histochemical analysis of ITGAM expression (macrophages). Histologic sections of aorta from the indicated animal groups were analyzed for ITGAM protein using anti-ITGAM antibody. Note that the AAV/hPRDX6-HCD treated animals displayed a much lower brown ITGAM signal than the AAV/Neo-HCD treated animals.

D. shows a similar analysis with anti-CD68 antibody, another marker of macrophages, with similar results as ITGAM.

can be seen, COL1A2 levels trended lower in hPRDX6-HCD treated animals than Neo-HCD treated. As nothing significant was found we did not analyze collagen expression further. However, clearly, hPRDX6 gene expression is not pro-fibrotic.

Discussion

These data demonstrate that hPRDX6 gene delivery by AAV2/8 using systemic tail vein injection is effective in both delivery and therapeutic effect. Atherosclerosis was inhibited by all parameters measured, including direct measurements of/within the aorta, QRT-PCR for macrophage markers, and immuno-histochemistry for macrophage markers. Moreover, no increase in collagen expression (fibrosis) was observed. As the biochemical activity of PRDX6 is well documented we did not attempt to remeasure its direct effect on thiol-specific ROS [29-32]. However the results show that the level of AAV-delivered hPRDX6 mRNA expression achieved was 1.7% that of β actin (Figure 1) at 20 weeks post virus injection and 20 weeks continuous HCD. While this may seem minimal expression, if one assumes that the average aortic cell (smooth muscle) translates the β actin and the hPRDX6 mRNAs at roughly the same efficiency and are roughly equivalent to the average cultured fibroblast [35], then a 1.7% expression level would result in, on average, approximately 2,600 hPRDX6 proteins being translated per minute per cell. However, this analysis doesn't take into account that the transduction level of AAV8 after 20 weeks will be less than 100%, nor the likelihood that smooth muscle cells express more βactin than fibroblasts. Therefore the level
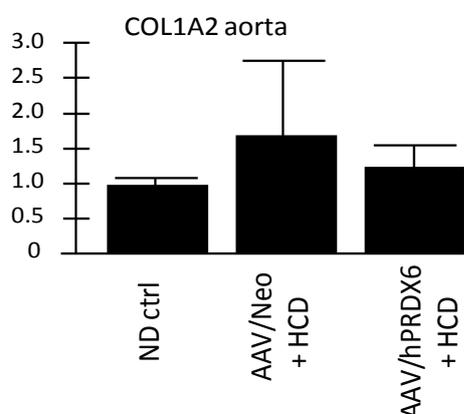
Figure 5: Collagen expression in the aortas. This figure shows a QRT-PCR analysis of COL1A2 expression in the aortas, a major marker of fibrosis. Note that COL1A2 levels trended lower in hPRDX6-HCD treated animals than Neo-HCD treated.

of hPRDX6 being produced specifically in AAV-transduced cells is likely to be higher than the 2,600 molecules per minute per cell just described. It should also be mentioned the AAV-delivered hPRDX6 expression augments that of the endogenous mouse PRDX6 already present (Figures 1C and 1D).

With this level of hPRDX6 expression aortic remodeling in response to HCD was minimized as shown in figure 2. This protection against atherosclerotic remodeling, and hPRDX6 therapeutic effect, was further verified by studying macrophage (foam cell) markers, either by QRT-PCR or immune-histochemistry. While our various data presented internally consistent, our data are not fully consistent with that reported by Phelan et al. in which they reported no protection against atherosclerosis in PRDX6 over-expressing transgenic mice [36]. Yet it can be seen that one paired set of PRDX6 transgenic mice within their study did trend toward a therapeutic effect, in table 1, Line 153 transgene – versus +, where the transgene (PRDX6) + phenotype trended to have a 20% small lesion area, but did not reach significance. However, this same research group reevaluated this issue, publishing the following year that the observance of therapeutic effect by PRDX6 was dependent upon the transgenic mouse background [37]. It should be pointed out that we are using the LDLR KO mouse which has proven itself as a reliable animal model of high cholesterol diet-induce atherosclerosis, with over 600 hits by pubmed search.

There are few reports on the effects of PRDX6 on the immune system or immune cells. In one report lower PRDX6 levels were associated with skin depigmentation, possibly autoimmunity, during DNA vaccine administration [38]. This is very minimal information, but suggests selective immune-suppression by PRDX6, possibly against cell mediated immunity. Most of our previous gene therapy treatments for atherosclerosis, in fact, targeted the immune system, lowering immune response, lowering immune cell activation (eg. using interleukin 10 [IL-10] gene delivery) [33] or change leukocyte accumulation (eg. induce Treg) [39]. There was a lack of any strong change of direction of the general immune status in the aorta affected by PRDX6 gene delivery (Figure 4). The cytokine profiles of IL-7 (Th1 cytokine), IL-12 (Th1), and IL-4 (Th2) were minimally changed. Only IL-10 (Th2) showed any significant change, being much lower in hPRDX6-treated animals than Neo-treated. Thus, from our perspective, hypothesizing that increased immune response is a major driver of atherogenesis, our findings on

PRDX6 were unexpected. However, while the cytokine profile was unremarkable, the level of aortic macrophages (foam cells) was still markedly lower in the hPRDX6-treated animals (Figure 3). This was confirmed by both QRT-PCR and immuno-histochemistry analysis for macrophage markers. We are unsure about how anti-thiol ROS activity and lower macrophage numbers might correlate. The correlation does not appear to be through traditional cytokine signaling. Thus while the specific mechanism of action is unclear, the success of AAV/hPRDX6 gene delivery in limiting atherogenesis in LDLR KO mice on HCD suggests that this approach has merit and should be further studied.

Acknowledgements

References

1. Aruoma OI, Halliwell B, Dizdaroglu M (1989) Iron ion-dependent modification of bases in DNA by the superoxide radical-generating system hypoxanthine/xanthine oxidase. J Biol Chem 264: 13024-13028.

2. Knight JA (1995) Diseases related to oxygen-derived free radicals. Ann Clin Lab Sci 25: 111-121.

3. Halliwell B, Gutteridge JM (1992) Biologically relevant metal ion-dependent hydroxyl radical generation. An update. FEBS Lett 307: 108-112.

4. Halliwell B, Gutteridge JM (1990) Role of free radicals and catalytic metal ions in human disease: an overview. Methods Enzymol 186: 1-85.

5. McMillan DC, Powell CL, Bowman ZS, Morrow JD, Jollow DJ (2005) Lipids versus proteins as major targets of pro-oxidant, direct-acting hemolytic agents. Toxicol Sci 88: 274-283.

6. Singh U, Jialal I (2006) Oxidative stress and atherosclerosis. Pathophysiology 13: 129-142.

7. Chen K, Keaney JF Jr (2012) Evolving concepts of oxidative stress and reactive oxygen species in cardiovascular disease. Curr Atheroscler Rep 14: 476-483.

8. Cai H, Harrison DG (2000) Endothelial dysfunction in cardiovascular diseases: the role of oxidant stress. Circ Res 87: 840-844.

9. Mehta JL, Rasouli N, Sinha AK, Molavi B (2006) Oxidative stress in diabetes: a mechanistic overview of its effects on atherogenesis and myocardial dysfunction. Int J Biochem Cell Biol 38: 794-803.

10. Chakravarthy U, Hayes RG, Stitt AW, McAuley E, Archer DB (1998) Constitutive nitric oxide synthase expression in retinal vascular endothelial cells is suppressed by high glucose and advanced glycation end products. Diabetes 47: 945-952.

11. Stephens NG, Parsons A, Schofield PM, Kelly F, Cheeseman K, et al. (1996) Randomised controlled trial of vitamin E in patients with coronary disease: Cambridge Heart Antioxidant Study (CHAOS) Lancet 347: 781-786.

12. Tardif JC, Côté G, Lespérance J, Bourassa M, Lambert J, et al. (1997) Probucol and multivitamins in the prevention of restenosis after coronary angioplasty. Multivitamins and Probucol Study Group. N Engl J Med 337: 365-372.

13. Niu K, Guo H, Kakizaki M, Cui Y, Ohmori-Matsuda K, et al. (2013) A tomato-rich diet is related to depressive symptoms among an elderly population aged 70 years and over: a population-based, cross-sectional analysis. J Affect Disord 144: 165-170.

14. Rifler JP, Lorcerie F, Durand P, Delmas D, Ragot K, et al. (2012) A moderate red wine intake improves blood lipid parameters and erythrocytes membrane fluidity in post myocardial infarct patients. Mol Nutr Food Res 56: 345-351.

15. Hermonat PL, Muzyczka N (1984) Use of adeno-associated virus as a mammalian DNA cloning vector: transduction of neomycin resistance into mammalian tissue culture cells. Proc Natl Acad Sci U S A 81: 6466-6470.

16. Tratschin JD, West MH, Sandbank T, Carter BJ (1984) A human parvovirus, adeno-associated virus, as a eucaryotic vector: transient expression and encapsidation of the procaryotic gene for chloramphenicol acetyltransferase. Mol Cell Biol 4: 2072-2081.

17. Hermonat PL, Labow MA, Wright R, Berns KI, Muzyczka N (1984) Genetics of adeno-associated virus: isolation and preliminary characterization of adeno-associated virus type 2 mutants. J Virol 51: 329-339.

18. Jiang H, Lillicrap D, Patarroyo-White S, Liu T, Qian X, et al. (2006) Multiyear therapeutic benefit of AAV serotypes 2, 6, and 8 delivering factor VIII to hemophilia A mice and dogs. Blood 108: 107-115.

19. Buchlis G, Podsakoff GM, Radu A, Hawk SM, Flake AW, et al. (2012) Factor IX expression in skeletal muscle of a severe hemophilia B patient 10 years after AAV-mediated gene transfer. Blood 119: 3038-3041.

20. Maksimenko AV (2005) Experimental antioxidant biotherapy for protection of the vascular wall by modified forms of superoxide dismutase and catalase. Curr Pharm Des 11: 2007-2016.

21. Levonen AL, Vähäkangas E, Koponen JK, Ylä-Herttuala S (2008) Antioxidant gene therapy for cardiovascular disease: current status and future perspectives. Circulation 117: 2142-2150.

22. Yan S, Brown SL, Kolozsvary A, Freytag SO, Lu M, et al. (2008) Mitigation of radiation-induced skin injury by AAV2-mediated MnSOD gene therapy. J Gene Med 10: 1012-1018.

23. Qi X, Sun L, Hauswirth WW, Lewin AS, Guy J (2007) Use of mitochondrial antioxidant defenses for rescue of cells with a Leber hereditary optic neuropathy-causing mutation. Arch Ophthalmol 125: 268-272.

24. Maksimenko AV, Vavaev AV (2012) Antioxidant enzymes as potential targets in cardioprotection and treatment of cardiovascular diseases. Enzyme antioxidants: the next stage of pharmacological counterwork to the oxidative stress. Heart Int 7: e3.

25. Bräsen JH, Leppänen O, Inkala M, Heikura T, Levin M, et al. (2007) Extracellular superoxide dismutase accelerates endothelial recovery and inhibits in-stent restenosis in stented atherosclerotic Watanabe heritable hyperlipidemic rabbit aorta. J. Am. Coll. Cardiol 50: 2249-2253.

26. Fennell JP, Brosnan MJ, Frater AJ, Hamilton CA, Alexander MY, et al. (2002) Adenovirus-mediated overexpression of extracellular superoxide dismutase improves endothelial dysfunction in a rat model of hypertension. Gene Ther 9: 110-117.

27. Barkats M, Bemelmans AP, Geoffroy MC, Robert JJ, Loquet I, et al. (1996) An adenovirus encoding CuZnSOD protects cultured striatal neurones against glutamate toxicity. Neuroreport 7: 497-501.

28. Hassett P, Curley GF, Contreras M, Masterson C, Higgins BD, et al. (2011) Overexpression of pulmonary extracellular superoxide dismutase attenuates endotoxin-induced acute lung injury. Intensive Care Med 37: 1680-1687.

29. Phelan SA, Johnson KA, Beier DR, Paigen B (1998) Characterization of the murine gene encoding Aop2 (antioxidant protein 2) and identification of two highly related genes. Genomics 54: 132-139.

30. Phelan SA (1999) AOP2 (antioxidant protein 2): structure and function of a unique thiol-specific antioxidant. Antioxid Redox Signal 1: 571-584.

31. Kondo N, Nakamura H, Masutani H, Yodoi J (2006) Redox regulation of human thioredoxin network. Antioxid Redox Signal 8: 1881-1890.

32. Yamada Y, Limmon GV, Zheng D, Li N, Li L, et al. (2012) Major shifts in the spatio-temporal distribution of lung antioxidant enzymes during influenza pneumonia. PLoS One 7: e31494.

33. Liu Y, Li D, Chen J, Xie J, Bandyopadhyay S, et al. (2006) Inhibition of atherogenesis in LDLR knockout mice by systemic delivery of adeno-associated virus type 2-hIL-10. Atherosclerosis 188: 19-27.

34. Khan JA, Cao M, Kang BY, Liu Y, Mehta JL, et al. (2010) AAV/hSTAT3-gene delivery lowers aortic inflammatory cell infiltration in LDLR KO mice on high cholesterol. Atherosclerosis 213: 59-66.

35. Kislauskis EH, Zhu X, Singer RH (1997) beta-Actin messenger RNA localization and protein synthesis augment cell motility. J Cell Biol 136: 1263-1270.

36. Phelan SA, Wang X, Wallbrandt P, Forsman-Semb K, Paigen B (2003) Overexpression of Prdx6 reduces H2O2 but does not prevent diet-induced atherosclerosis in the aortic root. Free Radic Biol Med 35: 1110-1120.

37. Wang X, Phelan SA, Petros C, Taylor EF, Ledinski G, et al. (2004) Peroxiredoxin 6 deficiency and atherosclerosis susceptibility in mice: significance of genetic background for assessing atherosclerosis. Atherosclerosis 177: 61-70.

38. Zhou Q, Wang F, Zhang Y, Yang F, Wang Y, et al. (2011) Down-regulation of Prdx6 contributes to DNA vaccine induced vitiligo in mice. Mol Biosyst 7: 809-816.

39. Khan JA, Cao M, Kang BY, Liu Y, Mehta JL, et al. (2011) Systemic human Netrin-1 gene delivery by adeno-associated virus type 8 alters leukocyte accumulation and atherogenesis in vivo. Gene Ther 18: 437-444.